Journal of Physics: Conference Series **775** (2016) 012003 doi:10.1088/1742-6596/775/1/012003

Non-Maxwellian background effects in gyrokinetic simulations with GENE

A. Di Siena[1], T. Görler[1], H. Doerk[1], J. Citrin[2,3],T. Johnson[4], M. Schneider[3], E. Poli[1] and JET Contributors[5]

[1]Max Planck Institute for Plasma Physics, Boltzmannstr.2, 85748 Garching, Germany
[2]FOM Institute DIFFER, PO Box 6336, 5600 HH Eindhoven, The Netherlands
[3]CEA, IRFM, F-13108 Saint Paul Lez Durance, France
[4]VR Association, EES, KTH, Stockholm, Sweden
[5]EUROfusion Consortium, JET, Culham Science Centre, Abingdon, OX14 3DB, UK

E-mail: adisi@ipp.mpg.de

Abstract. The interaction between fast particles and core turbulence has been established as a central issue for a tokamak reactor. Recent results predict significant enhancement of electromagnetic stabilisation of ITG turbulence in the presence of fast ions. However, most of these simulations were performed with the assumption of equivalent Maxwellian distributed particles, whereas to rigorously model fast ions, a non-Maxwellian background distribution function is needed. To this aim, the underlying equations in the gyrokinetic code GENE have been re-derived and implemented for a completely general background distribution function. After verification studies, a previous investigation on a particular JET plasma has been revised with linear simulations. The plasma is composed by Deuterium, electron, Carbon impurities, NBI fast Deuterium and ICRH ^{3}He. Fast particle distributions have been modelled with a number of different analytic choices in order to study the impact of non-Maxwellian distributions on the plasma turbulence: slowing down and anisotropic Maxwellian. Linear growth rates are studied as a function of the wave number and compared with those obtained using an equivalent Maxwellian. Generally, the choice of the ^{3}He distribution seems to have a stronger impact on the microinstabilities than that of the fast Deuterium.

1. Introduction

Developing a better understanding of the impact of fast particles on plasma core turbulence is an essential task for an improved performance assessment of future fusion reactors like ITER, where the energetic particles fraction is significant. In this work, the interaction between fast particles and plasma core turbulence is studied in the radially local limit. Therefore, energetic geodesic acoustic mode (EGAMs) effects will not be taken into account. However, the latter are usually negligible in the core plasma region [1]. In this context, recent experimental and computational results suggest positive and stabilising effects on the background turbulence, especially on the ITG modes [2, 3], typically considered as the most limiting microinstability in a tokamak reactor. In particular, fast ion dilution of the main ion species [4, 5], Shafranov shift stabilisation [6] as well as linear and nonlinear electromagnetic stabilisation in the presence of fast ions suprathermal pressure gradients [2, 7] have been proved to greatly stabilise the plasma core turbulence. Although some previous gyrokinetic studies could already well reproduce the experimental observation, the linear reduction of the growth rates and the nonlinear reduction

of the main ion heat flux are somewhat too strong such that the power balance was reached with R/L_{T_i} above the experimental values [8]. However, most of these simulations have been performed with the assumption of equivalent Maxwellian distributed particles, whereas it is well known that to rigorously model fast particles, a non-Maxwellian background distribution function is needed. Indeed, anisotropies and asymmetries in the fast particles distribution functions can, in principle, have some additional effects on the main plasma turbulence. For this reason, in this paper we present low beta electromagnetic simulations with non-Maxwellian fast particles distribution functions with the δf gyrokinetic code GENE [9]. The latter has been modified and generalised in order to include any number of analytic non-Maxellian fast particles species, namely slowing down and asymmetric and anisotropic Maxwellian, which as already mentioned, provide the most appropriate description. Linear electrostatic benchmarks against published results [10] obtained with GKW [11, 12] and GS2 [13, 14] are presented, which include slowing down fast particles in the electrostatic case. Furthermore, a relatively low beta JET plasma with both NBI and ICRH fast ions has been revised and analysed with linear simulations. Comparisons on the linear growth rates are shown in this paper between the different fast ion distribution functions and the previous Maxwellian results.

2. Theoretical background

2.1. Equilibrium distribution functions

All the simulations presented in this work have been carried out with the gyrokinetic δf code GENE, which solves numerically the nonlinear coupled Vlasov-Maxwell system of equations on a five dimensional grid for each time step. GENE can include full electromagnetic effects, realistic collisional operators as well as experimental geometries. The background distribution function usually considered in most of the gyrokinetic codes is a local Maxwellian (defined in Eq.(1)). The latter is a very good approximation for all the thermalised species, however, it lacks validity for fast particles where anisotropies and asymmetries cannot be described with a Maxwellian distribution function. In order to describe appropriately the dynamic of non thermalised particles, the gyrokinetic equations have been re-derived and implemented without doing any assumption on the background distribution function in the low-beta electromagnetic case, i.e. neglecting the parallel magnetic fluctuations ($B_{1,\shortparallel}$). This very flexible setup allows to implement and use a large variety of different distribution functions and study the impact of energetic particles on the plasma turbulence. In the present work the equilibrium distribution function F_0 for thermal electrons and ions has been modelled with a Maxwellian

$$F_{0,M} = \frac{n_0}{\pi^{3/2} v_{th}^3} \exp\left(\frac{-m v_{\shortparallel}^2/2 - \mu B_0}{T_0}\right) \tag{1}$$

Here, m is the particle mass, T_0 is the equilibrium temperature, n_0 particles density and $v_{th} = (2T_0/m)^{1/2}$ is the thermal velocity. The fast particle distributions have been modelled with a number of different analytic choices: slowing down [15] and an asymmetric and anisotropic Maxwellian [16]. The slowing down is a solution of the Fokker-Planck equation with an isotropic delta-function particle source and is defined as follow

$$F_{0,s} = \frac{3n_0}{4\pi \log\left(1 + \frac{v_\alpha^3}{v_c^3}\right)\left[v_c^3 + v^3\right]} \Theta\left(v_\alpha - v\right) \tag{2}$$

Here, the birth velocity is defined through the birth energy E_α in the following way $v_\alpha = (2E_\alpha/m_\alpha)^{1/2}$, while $v_c = v_{th,e}\left(\frac{3\sqrt{\pi}m_e}{4}\sum_{\text{main ions}}\frac{n_i z_i^2}{n_e m_i}\right)^{1/3}$ represents the critical slowing down velocity. Furthermore, Θ is the Heaviside step function. The asymmetric and anisotropic

Maxwellian distribution function is defined as follows

$$F_{0,aM} = \frac{n_0 \exp\left(-\frac{\mu B_0}{T_0}\right)}{\pi^{3/2}\left(v_{th,-}+v_{th,+}\right)v_{th,\perp}^2}\left\{\exp\left(-\frac{v_{\shortparallel}^2}{v_{th,-}^2}\right)\left[1-\Theta\left(v_{\shortparallel}\right)\right]+\exp\left(-\frac{v_{\shortparallel}^2}{v_{th,+}^2}\right)\Theta\left(v_{\shortparallel}\right)\right\} \quad (3)$$

Here, $T_{\shortparallel,+}$ and $T_{\shortparallel,-}$ are respectively the temperature associated to the particles with positive and negative parallel velocity, while $T_\perp$ is the perpendicular temperature. In the limit of $T_{\shortparallel,+} = T_{\shortparallel,-}$ Eq.(3) reduces to the bi-Maxwellian distribution function, which is often used to model ICRH fast ions. The latter will be used afterwards for modelling the fast ICRH ions in the linear simulations. Furthermore, if $T_{\shortparallel,+} = T_{\shortparallel,-} = T_\perp$ Eq.(3) turns into Eq.(1). The non-Maxwellian fast particles temperature has been defined in order to have the same kinetic pressure as the equivalent Maxwellian distribution function [17], namely

$$\int v^2 F_{non-M} dv = \int v^2 F_M dv$$

In the following session the derivation of the non-Maxwellian gyrokinetic equations is presented in the low-beta electromagnetic case.

2.2. Non-Maxwellian gyrokinetic Vlasov-Maxwell equations

In the present section the analytic derivation of the non-Maxwellian gyrokinetic equations is revised in the low-beta electromagnetic case without doing any assumptions on the background distribution function of the plasma species. As starting point, we write the Vlasov equation which determines the time evolution of the gyrocenter distribution function [18] $F = F\left(\vec{X}, v_{\shortparallel}, \mu\right)$

$$\frac{\partial F}{\partial t} + \left[v_{\shortparallel}\hat{b}_0 + \left(\vec{v}_E + \vec{v}_{\nabla B} + \vec{v}_c\right)\right]\cdot\left\{\vec{\nabla}F - \left[q\vec{\nabla}\bar{\phi}_1 + \frac{q}{c}\hat{b}_0\dot{\bar{A}}_{1,\shortparallel} + \mu\vec{\nabla}B_0\right]\frac{1}{mv_{\shortparallel}}\frac{\partial F}{\partial v_{\shortparallel}}\right\} = 0 \quad (4)$$

Here, respectively the curvature, the $E\times B$ and the ∇B drift velocities have been defined $\vec{v}_C = \frac{v_{\shortparallel}^2}{\Omega}\left(\vec{\nabla}\times\hat{b}_0\right)_\perp$, $\vec{v}_E = \frac{c}{B_0^2}\left(\vec{B}_0\times\vec{\nabla}\xi_1\right)$ and $\vec{v}_{\nabla B_0} = \frac{\mu c}{qB_0^2}\left(\vec{B}_0\times\vec{\nabla}B_0\right)$; ξ_1 represents the modified potential $\xi_1 = \bar{\phi}_1 - \frac{v_{\shortparallel}}{c}\bar{A}_{1,\shortparallel}$; $\Omega = \frac{qB_0}{m}$ and $\hat{b}_0 = \frac{\vec{B}_0}{B_0}$. The over bar denotes gyro averaged quantities, which in the local code approximation reduces to the mere multiplication of the zero order Bessel function, i.e. $\bar{\phi}_1 = J_0\left(\lambda\right)\phi_1$; $\bar{A}_{1,\shortparallel} = J_0\left(\lambda\right)A_{1,\shortparallel}$; where $\lambda = \frac{k_\perp}{\Omega}(\frac{2B_0\mu}{m})^{1/2}$. In terms of computational effort it is convenient to split the gyrocenter distribution function in an equilibrium part F_0 and a small perturbation term F_1, with $F_1 \ll F_0$. The turbulent evolution of the system is then determined within the so-called δf-ordering of Eq.(4) which for a field aligned coordinate system can be rewritten in terms of the metric coefficients $g^{ij} = \nabla u^i\cdot\nabla u^j$ (with $u^i = (x,y,z)$, x radial direction, y poloidal direction, z toroidal direction) in the following way

$$\frac{\partial g_1}{\partial t} + \frac{C}{JB_0}\left\{v_{\shortparallel}\partial_z F_1 - \left(\frac{q}{m}\partial_z\phi_1\frac{\partial F_0}{\partial v_{\shortparallel}} + \frac{\mu}{m}\partial_z B_0\frac{\partial F_1}{\partial v_{\shortparallel}}\right)\right\} +$$

$$+\frac{cB_0}{CB^*_{o,\shortparallel}}\left(\frac{g^{1i}g^{2j}-g^{2i}g^{1j}}{\gamma_1}\right)\left\{\left[\partial_i\xi_1 + \frac{\mu}{q}\partial_i B_0 + \frac{v_{\shortparallel}^2 m}{q}\left(\frac{\partial_i B_0}{B_0} + \frac{\beta_p}{2}\frac{\partial_i p_0}{p_0}\right)\right]\right.$$

$$\left.\left[\partial_j F_0 + \partial_j F_1 - \left(q\partial_j\phi_1 + \mu\partial_j B_0\right)\frac{1}{mv_{\shortparallel}}\frac{\partial F_0}{\partial v_{\shortparallel}}\right]\right\} = 0 \quad (5)$$

a modified distribution function $g_1 = F_1 - \frac{q}{mc}\bar{A}_{1,\shortparallel}\frac{\partial F_0}{\partial v_{\shortparallel}}$ has been introduced. C is defined below. In order to solve numerically Eq.(5) we need to derive a dimensionless equation. With this aim,

all the physical quantities have been split into a dimensionless value and a dimensional reference part. The reference value used to normalise Eq.(5) are the elementary electron charge e, the main ions mass m_i and temperature T_i, a reference magnetic field $B_{\rm ref}$ and a macroscopic length $L_{\rm ref}$. The normalised Vlasov equation for a completely general background distribution function can be written as

$$\begin{aligned}\frac{\partial g_1}{\partial t} = &-\frac{C}{JB_0}v_{th}v_{\shortparallel}\left[\partial_z F_1 - \frac{q}{2T_0 v_{\shortparallel}}\partial_z\phi_1\frac{\partial F_0}{\partial v_{\shortparallel}}\right] + \frac{C}{JB_0}v_{th}\frac{\mu}{2}\partial_z B_0\frac{\partial F_1}{\partial v_{\shortparallel}} + \\ &+\frac{T_0}{q}\left(\frac{\mu B_0 + mv_{\shortparallel}^2}{B_0}\right)\mathcal{K}_x\hat{\partial}_x F_0 - \frac{T_0}{q}\left[\left(\frac{\mu B_0 + mv_{\shortparallel}^2}{B_0}\right)\mathcal{K}_y - \frac{1}{C}\frac{v_{\shortparallel}^2\beta_{ref}}{B_0^2}\omega_p\right]\partial_y g_1 + \\ &+\left[\frac{1}{2v_{\shortparallel}}\frac{\partial F_0}{\partial v_{\shortparallel}}\left(\frac{\mu B_0 + mv_{\shortparallel}^2}{B_0}\right)\mathcal{K}_y - \frac{1}{C}\frac{v_{\shortparallel}^2\beta_{ref}}{B_0^2}\omega_p\frac{1}{2v_{\shortparallel}}\frac{\partial F_0}{\partial v_{\shortparallel}} - \frac{1}{C}\hat{\partial}_x F_0\right]\partial_y\xi_1 + \\ &-\frac{T_0}{q}\left(\frac{\mu B_0 + mv_{\shortparallel}^2}{B_0}\right)\mathcal{K}_x\partial_x g_1 + \frac{1}{2v_{\shortparallel}}\frac{\partial F_0}{\partial v_{\shortparallel}}\left(\frac{\mu B_0 + mv_{\shortparallel}^2}{B_0}\right)\mathcal{K}_x\partial_x\xi_1 + \\ &-\frac{1}{C}\left[\partial_x\xi_1\partial_y g_1 - \partial_y\xi_1\partial_x g_1\right] \end{aligned} \tag{6}$$

where we have defined the following geometrical coefficients $\mathcal{K}_x = -\frac{1}{C}\left(\partial_y B_0 - \frac{\gamma_3}{\gamma_1}\partial_z B_0\right)$, $\mathcal{K}_y = \frac{1}{C}\left(\partial_x B_0 - \frac{\gamma_3}{\gamma_1}\partial_z B_0\right)$, $\gamma_1 = g^{11}g^{22} - g^{21}g^{12}$, $\gamma_3 = g^{12}g^{23} - g^{22}g^{13}$ and $C = B_0/\gamma_1^{1/2}$; the normalised background pressure gradient $\omega_p = -\mathcal{L}_{\rm ref}\frac{\partial_x p_0}{n_{\rm ref}T_{\rm ref}}$ and the reference thermal to magnetic pressure ratio $\beta_{\rm ref} = \frac{8\pi n_{\rm ref}T_{\rm ref}}{B_{\rm ref}^2}$. If the equilibrium distribution function F_0 is chosen to be a local Maxwellian, one can show that Eq.(6) reduces to the well-known gyrokinetic equation known in literature see, e.g., Ref.[18].

2.3. Velocity space moments

In order to treat self-consistently our fluctuating system it is necessary to derive the fluctuating component of the electromagnetic fields from the perturbed distribution function. In this section the evaluation of the general moment of the perturbed distribution function

$$M_{a,b}\left(\vec{x}\right) = \int f\left(\vec{x},\vec{v}\right)v_{\shortparallel}^a v_{\perp}^b d^3v$$

is established. Since, from the Vlasov equation we can evaluate the time evolution of the gyrocenter distribution function it is convenient to transform the integrand of the general velocity moment equation in terms of the gyrocenter coordinates:

$$M_{a,b}\left(\vec{x}\right) = \int \delta\left(\vec{X} + \vec{r} - \vec{x}\right)T^* F_1\frac{B_0\left(\vec{X}\right)}{m}v_{\shortparallel}^a v_{\perp}^b d^3X dv_{\shortparallel}d\mu d\theta$$

where $\vec{r}$ is the gyroradius vector and T^* is the pull back operator, which acts on the perturbed distribution function in the following way

$$\begin{aligned}T^* F_1 = F_1 + \frac{1}{B_0}\Bigg\{&\left(\Omega\frac{\partial F_0}{\partial v_{\shortparallel}} - \frac{q}{c}v_{\shortparallel}\frac{\partial F_0}{\partial\mu}\right)\cdot\left(\vec{A}_1\left(\vec{X}+\vec{r}\right) - \bar{\vec{A}}_1\left(\vec{X}\right)\right) \\ &+q\left(\phi_1\left(\vec{X}+\vec{r}\right) - \bar{\phi}_1\left(\vec{X}\right)\right)\frac{\partial F_0}{\partial\mu}\Bigg\}\end{aligned}$$

Performing the integrals over θ and $\vec{X}$ it is straightforward to show that the generic moment of our gyrocenter distribution function can be reduced to

$$M_{a,b}\left(\vec{x}\right)=\frac{2\pi}{m}\int B_0\left(\vec{x}\right)\left\{\left\langle F_1\left(\vec{x}-\vec{r}\right)\right\rangle+\frac{1}{B_0\left(\vec{x}\right)}\left[\left(\Omega\frac{\partial F_0}{\partial v_{\shortparallel}}-\frac{q}{c}v_{\shortparallel}\frac{\partial F_0}{\partial\mu}\right)\cdot\left(\vec{A}_1\left(\vec{x}\right)-\left\langle\bar{\vec{A}}_1\left(\vec{x}-\vec{r}\right)\right\rangle\right)+\right.\right.$$
$$\left.\left.+q\left(\phi_1\left(\vec{x}\right)-\left\langle\bar{\phi}_1\left(\vec{x}-\vec{r}\right)\right\rangle\right)\frac{\partial F_0}{\partial\mu}\right]\right\}v_{\shortparallel}^a v_{\perp}^b dv_{\shortparallel}d\mu \tag{7}$$

Here, the brackets $\langle\ldots\rangle$ denote the θ integrated function, i.e. gyroaveraged quantities. In case of a background Maxwellian distribution function, the generic moment equation can be greatly simplified. Indeed, the terms that multiply the vector potential cancel and the $v_{\shortparallel}$-integration can be performed analytically.

2.4. Field equations

The Poisson equation and the Ampere's law for both the parallel and perpendicular component of the electromagnetic potential can be written in terms of the $M_{0,0}$ and $M_{1,0}$ moments of the perturbed distribution function

$$\nabla_{\perp}^2\phi_1\left(\vec{x}\right)=-4\pi\sum_j q_j n_{1,j}\left(\vec{x}\right)=-4\pi\sum_j q_j M_{0,0,j}\left(\vec{x}\right)$$

$$-\nabla_{\perp}^2 A_{1,\shortparallel}\left(\vec{x}\right)=\frac{4\pi}{c}\sum_j j_{\shortparallel,1,j}\left(\vec{x}\right)=\frac{4\pi}{c}q_j M_{1,0,j}\left(\vec{x}\right)$$

where we used the following Cartesian coordinate system $\left(\hat{e}_1,\hat{e}_2,\hat{b}_0\right)$.

From Eq.(7) the normalised non-Maxwellian field equations become

$$P\phi_1\left(\vec{x}\right)+\mathcal{F}A_{1,\shortparallel}\left(\vec{x}\right)=q\pi n_0 B_0\int J_0\left(\lambda\right)g_1 dv_{\shortparallel}d\mu$$

$$\mathcal{H}A_{1,\shortparallel}\left(\mathbf{x}\right)+\mathcal{L}\phi_1\left(\vec{x}\right)=qn_0\pi\beta_{ref}\frac{B_0 v_{th}}{2}\int v_{\shortparallel}J_0 g_1 dv_{\shortparallel}d\mu$$

Here, we have introduced the following operators

$$P=k_{\perp}^2\lambda_{De}^2-\frac{\pi q^2 n_0}{T_0}\int\left(1-J_0^2\right)\frac{\partial F_0}{\partial\mu}dv_{\shortparallel}d\mu\qquad\mathcal{F}=\frac{2\pi q^2 n_0}{m v_{th}}\int\left[\left(1-J_0^2\right)v_{\shortparallel}\frac{\partial F_0}{\partial\mu}-\frac{B_0}{2}\frac{\partial F_0}{\partial v_{\shortparallel}}\right]dv_{\shortparallel}d\mu$$

$$\mathcal{H}=k_{\perp}^2-\frac{q^2 n_0\pi\beta_{ref}}{m}\int\left[B_0\frac{v_{\shortparallel}}{2}\frac{\partial F_0}{\partial v_{\shortparallel}}-v_{\shortparallel}^2\frac{\partial F_0}{\partial\mu}\left(1-J_0^2\right)\right]dv_{\shortparallel}d\mu$$

$$\mathcal{L}=\frac{q^2 n_0\pi\beta_{ref}}{m v_{th}}\int\frac{\partial F_0}{\partial\mu}\left(1-J_0^2\right)v_{\shortparallel}dv_{\shortparallel}d\mu$$

It is worth noting that for a completely general background distribution function the field equations constitute a system of coupled equations. This system decouples if a Maxwellian distribution function is chosen.

3. Linear simulations

In this paragraph linear electrostatic benchmarks are shown with GS2 and GKW for slowing down fast particles to verify the results shown in the previous section. Furthermore, the relevance of fast particles on the ITG turbulence in a JET hybrid scenario [8] and low magnetic shear ($\hat{s}=0.5$) has been studied with linear simulations.

3.1. Verification

Linear electrostatic benchmarks have been carried out with the gyrokinetic code GS2 and GKW in order to prove the correctness of the derivation and implementation of the non-Maxwellian Vlasov-Maxwell system of equations. Both these codes have published results from simulations with a slowing-down equilibrium distribution function for a single fast particle species [10]. In this paragraph, growth rates as a function of the fast particle concentration and the alpha particle diffusivity as a function of the electron temperature are shown in Fig.(1) for the same reference case as the one studied in Ref.[10], i.e. cyclone base for a Deuterium, electron and alpha particle plasma. The input parameters are briefly summarised in the following table. As can be seen from Fig.(1) the agreements between codes is excellent. These results prove the validity of both the analytic calculation and the numerical implementation.

$\hat{s}$	q	T_e/T_i	R/L_{T_i}	R/L_{T_e}	R/L_{n_e}	r/a	R/a
0.8	1.4	1.0	6.0	6.0	3.0	0.5	3.0

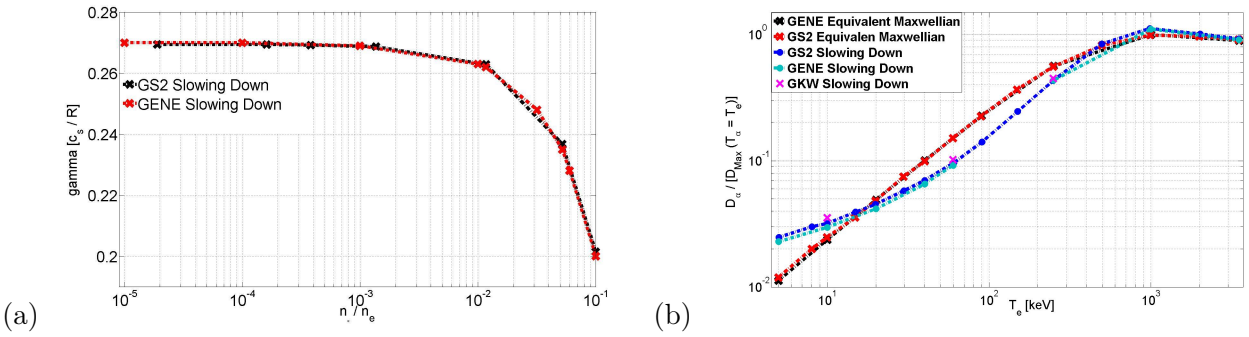

Figure 1: (a) GENE (red line) and GS2 (black line) growth rates as a function of the α particles density concentration plotted in logarithmic scale. (b) GENE (cyan line), GS2 (blue line) and GKW (magenta cross) α particles diffusivity for slowing down distribution function and GENE (black line), GS2 (red line) α particles diffusivity for equivalent Maxwellian distribution function normalised to the diffusivity of thermal helium plotted in logarithmic scale.

3.2. Microinstability study including more realistic background

In this section a particular JET plasma is revised and analysed with linear simulations [8]. The bulk plasma is composed by Deuterium, electron and Carbon impurities, while the fast particles are fast Deuterium (from NBI) and ^{3}He (from minority heating). The fast ion background distribution function has been modelled with a slowing down, an equivalent Maxwellian and with an asymmetric and anisotropic Maxwellian, in order to study the impact of non Maxwellian background distribution functions on the ITG instability. Low beta electromagnetic effects, collisions, impurities, fast ions, and experimental geometry are included. In the following tables the background plasma and magnetic geometry as well as the fast particles parameters are summarised.

$\hat{s}$	q	T_e/T_i	R/L_{T_i}	R/L_{T_e}	R/L_{n_e}	β_e [%]	ν^*
0.5	1.7	1.0	10	6.8	1.3	0.33	0.038

n_{fD}	$n_{^3He}$	T_{fD}	$T_{^3He}$	$R/L_{T_{fD}}$	$R/L_{T_{^3He}}$	R/L_{nfD}	$R/L_{n_{^3He}}$
0.06	0.07	9.8	6.9	3	20	13	1.5

3.2.1. Slowing down background In order to study the impact of the fast ion background distribution on microinstabilities in a realistic scenario, we performed linear simulations with five species, modelling the fast particles with a slowing down (defined in Eq.(2)). In Fig.2 linear growth rates are shown for four different cases: equivalent Maxwellian fast particles, slowing down fast particles, slowing down fast Deuterium - Maxwellian ^{3}He and without fast particles (3 species).

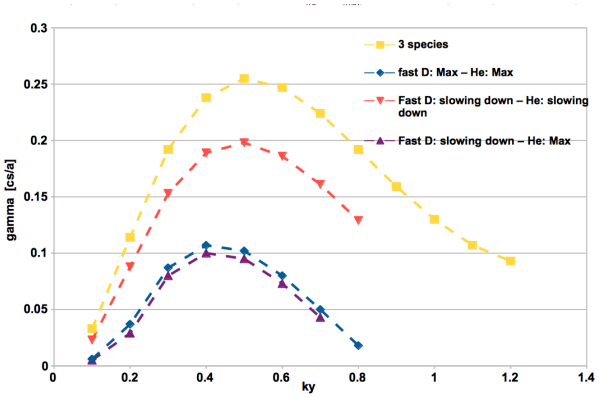

Figure 2: Linear growth rates as function of $k_y\rho_i$ for equivalent Maxwellian fast particles (blue line); Slowing down fast particles (yellow line); Slowing down fast Deuterium - equivalent Maxwellian ^{3}He (green line); without fast particles (red line).

The electromagnetic stabilisation is stronger for the equivalent Maxwellian fast ions simulations, whose growth rates are $\sim 50\%$ lower than the slowing down ones. The most unstable mode is slightly shifted to higher k_y for the slowing down case, matching the k_y related to the most unstable mode in the three species simulation. From the comparison between the slowing down fast Deuterium - equivalent Maxwellian ^{3}He and the both slowing down fast particles growth rates, it is possible to see that the main difference arises when the ^{3}He is modelled with a slowing down distribution. The slowing down fast Deuterium results are slightly more stable than the equivalent Maxwellian ones, while the ^{3}He has an opposite behavior. Slowing down ^{3}He growth rates are much more unstable than the ones carried out using an equivalent Maxwellian. However, a slowing-down distribution function is most likely a poor approximation for the ^{3}He species.

3.2.2. Bi-Maxwellian background In this section we compare the results carried out with the equivalent Maxwellian and the bi-Maxwellian distributions. The latter can be carried out from Eq.(3) in the limit of $T_{\shortparallel,+} = T_{\shortparallel,-}$ and is considered as a first order approximation for the ICRH-driven fast ^{3}He [19]. The ^{3}He profiles, i.e. both temperatures and temperature gradients, were extracted from the SPOT/SELFO code [20, 21]. In Fig.3 linear growth rates are shown as a

function of $k_y\rho_i$ for five species simulations. The fast Deuterium is modelled with the equivalent Maxwellian distribution function, while for the fast ^{3}He we used the bi-Maxwellian distribution function.

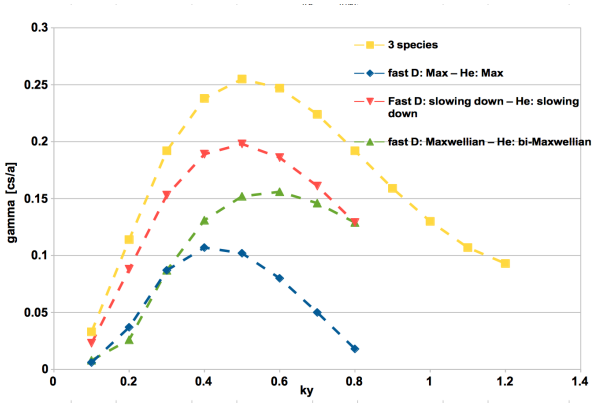

Figure 3: Linear growth rates as function of $k_y\rho_i$ for equivalent Maxwellian fast particles (blue line); Slowing down fast particles (red line); equivalent Maxwellian fast Deuterium - Bi-Maxwellian ^{3}He (green line); without fast particles (yellow line).

As can be seen in Fig.3 the strength of the electromagnetic stabilisation is decreased when modelling the ^{3}He distribution with the bi-Maxwellian. The growth rates are higher than the equivalent Maxwellian ones. In particular, it is worth noting that the difference between the equivalent Maxwellian and bi-Maxwellian growth rates increases with k_y. From Fig.2 and Fig.3 it is possible to observe that the ^{3}He background distribution has a much stronger effect on the plasma mictroturbulence than that of the fast Deuterium.

4. Conclusions

The gyrokinetic turbulence code GENE has been modified and extended in the low-beta electromagnetic case in order to treat any number of non-Maxwellian fast particle species. In particular, slowing down and asymmetric and anisotropic Maxwellian fast particles can now be studied. In order to test and verify the implementation, linear electrostatic benchmarks have been shown for slowing down fusion born alpha particles with existing data from the gyrokinetic codes GS2 and GKW. After these verification studies, a previous equivalent Maxwellian study on a particular JET plasma with fast ion enhanced electromagnetic stabilisation has been revised and analysed with linear simulations. The bulk plasma is composed by Deuterium, electron and Carbon impurities, while the fast particles are NBI fast Deuterium and ICRH ^{3}He. Electromagnetic effects, collisions and experimental geometry have been included. In this context, linear growth rates are studied as a function of the wave number and compared with those obtained using an equivalent Maxwellian. It has been found that also with the more realistic distribution function the increased EM-stabilisation with fast ions still holds, even if the strength of the effect with ICRH is slightly weaker. Furthermore, a lack of sensitivity to the NBI fast ion distribution has been observed. Generally, it has been found that the choice of the ^{3}He background distribution has a stronger impact on the linear results than the fast Deuterium background. These results would be in line with the previous nonlinear findings where gradients higher than the nominal ones had to be employed in order to match the experimental heat fluxes [7, 8]. A corresponding nonlinear analysis will be performed in the near future.

Acknowledgments
The simulations presented in this work were carried out using the TOKP cluster at the Rechenzentrum Garching (RZG), Germany. This work has furthermore been carried out within the framework of the EUROfusion Consortium and has received funding from the Euratom research and training programme 2014-2018 under grant agreement No 633053. The views and opinions expressed herein do not necessarily reflect those of the European Commission.

References
[1] D. Zarzoso et al. 2013 *Phys. Rev. Lett.* **110** 125002
[2] M. Romanelli et al. 2010 *Plasma Physics and Controlled Fusion* **52** 4
[3] J. Garcia et al. 2015 *Nuclear Fusion* **55** 5
[4] G. Tardini et al. 2007 *Nucl. Fusion* **47** 280
[5] C. Holland et al. 2011 *Phys. Plasmas* **18** 056113
[6] C. Bourdelle et al. 2005 *Nucl. Fusion* **45** 110
[7] J. Citrin et al. 2015 *Plasma Physics and Controlled Fusion* **57** 014032
[8] J. Citrin et al. 2013 *Phys. Rev. Lett.* **111** 155001
[9] F. Jenko et al. 2000 *Phys. Plasmas* **7** 1904; See http://genecode.org for code details and access
[10] C. Angioni et al. 2008 *Phys. Plasmas* **15**, 052307
[11] A. G. Peeters et al. 2004 *Phys. Plasmas* **11**, 3748
[12] A. G. Peeters et al. 2009 *Comput. Phys. Commun.* **180**, 2650
[13] M. Kotschenreuther et al. 1995 *Comput. Phys. Commun.* **88**, 128
[14] W. Dorland et al. 2000 *Phys. Rev. Lett.* **85**, 5579
[15] J. Gaffey 1976 *J.Plasma Phyisics* **16** part 2
[16] T. Dannert et al. 2008 *Phys. Plasmas* **15** 062508
[17] Estrada-Mila et al. 2006 *Phys. Plasmas* **13** 112303
[18] A.J. Brizard and T. S. Hahm 2007 *Rev. Modern Physics* **79** 421
[19] R. O. Dendy et al. 1995 *Phys. Plasmas* **2**, 1623
[20] M. Schneider et al. 2011 *Nucl. Fusion* **51**, 063019
[21] J. Hedin et al. 2002 *Nucl. Fusion* **42**, 527